Research Papers
Issue RP0186
December 2013

ISC - Impacts on Soil and Coasts Division

Evaluation of climate driven simulations of Po river flow from 1971 to 2000 through flow-duration curve indices: preliminary results

By **Renata Vezzoli**[1]
1 Impacts on Soil and Coasts Division, CMCC
renata.vezzoli@cmcc.it

Paola Mercogliano[1,2]
2 Division Meteo System & Instrumentation Laboratory, C.I.R.A.
paola.mercogliano@cmcc.it

Silvano Pecora[3]
3 Servizio IdroMeteoClima Area Idrologia, ARPA Emilia-Romagna
specora@arpa.emr.it

Myriam Montesarchio[1]
myriam.montesarchio@cmcc.it

Alessandra Lucia Zollo[1]
alessandra.zollo@cmcc.it

Mauro Del Longo[3]
mdellongo@arpa.emr.it

and **Fabrizio Tonelli**[3]
ftonelli@arpa.emr.it

The present research paper collects the outcomes of activities carried out in the framework of Work Package 6.2.17 of the GEMINA project, funded by the Italian Ministry of Education, University and Research and the Italian Ministry of Environment, Land and Sea. The authors would also like to thank NEXTDATA project for supporting this research.

SUMMARY Climate shows a natural variability that influences the dynamics of river discharges. In particular, intense precipitations would cause floods, while prolonged dry periods are associated to droughts phenomena. In the Mediterranean area, climate change is expected to increase the frequency of these phenomena due to variations in the precipitation partitioning in both space and time. To evaluate the impacts of these changes on the Po river daily discharges, we have developed a modelling chain that includes both climate and hydrological models. The performances of the chain are currently under testing through different simulations over the period 1971-2000. These simulations are driven by precipitation and temperature from a high resolution observed climate dataset and from the regional climate model COSMO-CLM, driven by perfect boundary conditions given by ERA40 Reanalysis and by suboptimal boundary conditions, using the global climate model CMCC-CM. The aim of these simulations is to investigate the uncertainties introduced by the components of the modelling chain and their effects on simulated discharges: the first simulation is used as reference simulation, the second one aims to evaluate how the uncertainties, introduced by the RCM, COSMO-CLM, propagate to the simulated discharges; and the last one is designed to evaluate the joint effects of the GCM, CMCC-CM, and the RCM on the simulation outputs. The results of such analysis will be used to qualify the XXI century climate projections and to correctly interpret climate change impacts on hydrological cycle in the future. The simulations performances are evaluated by comparing the precipitation and discharge seasonality and through five indices based on the flow-duration curve, that is representative of the probability distribution function of the river flow. To improve the simulation results a quantile-quantile correction is applied to simulated discharges using 1972-1990 data as calibration period and validating the results on 1991-2000. The quantile-quantile corrected simulations better resemble discharge seasonality and flow-duration curve. Results show how probabilistic bias correction helps in reducing the overall uncertainty.

Keywords: Regional climate model, River discharge, Numerical simulations, Quantile-quantile correction, Flow-duration curve indices

INTRODUCTION

In the Mediterranean area most of climate models agree in expecting an increase in the frequency of extreme precipitation events but the intensity should be unchanged, and, in average, the total precipitation would decrease [5]. The foreseen different partitioning of precipitation will enhance the possibility of alternations between long dry periods and others short and extremely wet, this alternation will contribute to increase the hydrological vulnerability of the territory [2]. The effects of climate change on floods and droughts have been recently addressed by [2, 6, 10, 7, 18, 19, 16, 17] and at European level (for floods) by the Directive 2007/60/EC of the European Parliament and of the Council. The European Directive deals with the assessment and management of flood risk, and the reduction of its adverse consequences recognizing the role of both anthropogenic activities and climate change forcings. In Italy, vulnerability to precipitation partitioning is emphasised by the presence of several small catchments that tend to quickly overflow in response to heavy rainfall, even of short duration, and by the high urbanization rate of areas close to the rivers. To investigate the impacts of climate change on river flow regime we set up a climate/hydrological modelling chain that provides daily discharges of Po river and its tributaries. The case study was individuated in the Po river because of its national relevance, dimensions, availability of observations, and the increased severity of floods and droughts events experienced in the last decades [26]. In addition an already calibrated and validated hydrological/hydraulic chain is available at the Hydro-Meteo-Climate Service of the Regional Agency for Prevention and Environment (ARPA SIMC) of Emilia-Romagna Region in North Italy [3].

METHODOLOGY AND MODELS

Among the objectives of GEMINA project [27] there is the study of climate change impacts on extreme hydrological phenomena like droughts and floods, with particular attention to the Po river (Fig.1). For this reason a climate/hydrological modelling chain to simulate past (1971-2000) and future (2001-2100) discharges has been developed. Simulations referring to 1971-2000 are intended to evaluate the overall uncertainty associated to the different climate configurations before of investigating the impact of climate change on flood/drought hazard across the XXI century and the Po river adaptability to them. Table 1 summarises the climate simulations which will be considered within GEMINA project [27] for the present (1971-2000) on the left and the future (2001-2100) on the right.

The climate/hydrological modelling chain is composed in cascade by a climate module, i.e. precipitation and 2 meter temperature, and a hydrological/hydraulic module to simulate the climate impacts at the soil. The hydrological/hydraulic part of the modelling chain is common to all the simulations and it is composed by a physically based and spatially distributed hydrological model implemented in the software TOPKAPI (TOPographic Kinematic Approximation and Integration [12]) that estimates the different components of the rainfall-runoff transformation and provides the runoff to be used as input to a water balance model at basin scale implemented in the RIBASIM (RIver BAsin SIMulation [11]) software that simulates average daily discharges at different sections of the river network. The simulations listed on the left side of Tab.1 are relative to the period 1971-2000 and are driven by different climate datasets. The first one uses as climate inputs daily observed data gridded at the same resolution of the regional climate model COSMO-CLM

Table 1
Climate inputs to the hydrological component of the modelling chain. Left column refers to the period 1971-2000, the right column to the period 2001-2100.

Period 1971-2000	Period 2001-2100
High resolution atmospherical observed dataset	COSMO-CLM driven by CMCC-CM GCM (IPCC RCP4.5)
Run1: COSMO-CLM driven by ERA40 Reanalysis	COSMO-CLM driven by CMCC-CM GCM (IPCC RCP4.5) + statistical downscaling
Run2: COSMO-CLM driven by ERA40 Reanalysis + statistical downscaling	COSMO-CLM driven by CMCC-CM GCM (IPCC RCP8.5)
Run3: COSMO-CLM driven by CMCC-CM GCM	COSMO-CLM driven by CMCC-CM GCM (IPCC RCP8.5) + statistical downscaling
Run4: COSMO-CLM driven by CMCC-CM GCM + statistical downscaling	Other simulations to be scheduled

(about 0.0715° i.e. about 8 km); the precipitation field has been provided by ARPA SIMC on the basis of data published on Part I of Hydrological Yearbooks, while temperature is based on EOBS dataset [8], ARPA SIMC provides also additional information based on Part I of Hydrological Yearbooks on the temperature field for the period 1991-2010. For Po river basin, the Hydrological Yearbooks until 1991 are available on the websites of Italian Institute for Environmental Protection and Research (ISPRA) and of ARPA Emilia-Romagna with data relative to Emilia-Romagna region updated at 2012. The second and the third simulation are driven by the precipitation and temperature fields from COSMO-CLM [14] with ERA40 Reanalysis as boundary conditions [24]. The nominal resolution of ERA40 Reanalysis is 1.125° (about 128 km). In the third simulation the precipitation field has been statistically correct using the MOS Analogs technique [20, 21, 23] to improve the similarity between observed and simulated precipitation, thus it differs from the one used in the second simulation. The fourth simulation, covering the period 1971-2000, has the global climate model (GCM) CMCC-CM [15] as boundary conditions to the RCM COSMO-CLM. The GCM CMCC-CM is characterized by a nominal resolution of 0.75° (about 85 km). A detailed description of the regional climate model (RCM) COSMO-CLM and its validation when driven by ERA40 Reanalysis or CMCC-CM is available in [13, 28]. For the period 2001-2100, the IPCC Representative Concentration Pathways (RCP) 4.5 and 8.5 will be used as scenarios. RCP4.5 is a stabilization scenario where the total radiation forcing stabilized at 4.5 W/m^2 before 2100, while in RCP8.5 scenario the radiation forcing is still increasing in 2100 and emissions are higher [1].

In this Research Paper, we present a comparison among the discharges simulated using the climate fields presented above and listed on the left of Tab.1 as forcing to the hydrological and basin balance models. The first hydrological/hydraulic simulation, alternatively named Run1, is driven by the observed climate and the resulting discharges are the reference one. The choice of using a reference timeseries instead of observed discharges is justified by the changes in land use, water demand and management occurred in Po river basin in the last 30 years. A detailed knowledge of land use and water management actions in the past is required to correctly reproduce the observed discharges, however such information are available, in details, only for the last decade, thus the hydrological and hydraulic models are calibrated on such period. For this reason, a reference simulation is required for comparison. The second simulation, Run2, aims to evaluate how uncertainties introduced by COSMO-CLM affect the simulated discharges; the third one, Run3, wants to estimate if a statistical correction of the precipitation field is sufficient to remove/reduce the uncertainties introduced by the RCM. [21, 23] give a comparison among the capability of different statistical downscaling techniques, including MOS Analogs, to improve the similarity between the precipitation field obtained from COSMO-CLM with ERA40 Reanalysis as boundary conditions and the observed one. The fourth simulation, Run4, considered here is designed to evaluate the joint impact of suboptimal boundary condition, the GCM CMCC-CM, and of dynamically downscaling model, the RCM COSMO-CLM, on the simulated discharges. This last configuration is the one that will be used to study the climate change impacts on the hydrological hazard in the XXI century (right side of Tab.1). The fourth simulation will help also into interpret the simulated discharges under climate change scenarios. If the chosen RCM and/or GCM is changed the uncertainty introduced needs to be quantify from scratch.

The comparison among the precipitation fields over the period 1972-2000 (1971 is the spin-off year for the modelling chain and is neglecting in all the analysis) is presented in terms of monthly average areal precipitation in Fig.2(a). The comparison among the discharges over the same period is based on monthly values, Fig.2(b), and flow-duration curves, Fig.2(c). The flow-duration curve (hereinfter FDC) gives the exceedance probability $p = 1 - F$ for any discharge value and F is the cumulative probability associated to the discharges. The similarity among of the main features of the FDCs is evaluated through five indices introduced by [25] and applied with some minor modifications by [9, 4]. The indices are defined as:

- RQ1, bias in the mean value of FDC:

$$RQ1 = \frac{E[Q_J]}{E[Q_1]} - 1, \qquad (1)$$

  where $E[Q]$ indicates the average discharge simulated in RunJ with J=2,3,4.

- RQ2, bias in the median of FDC and is defined similarly to RQ1 following [4]

$$RQ2 = \frac{q_J(p = 0.5)}{q_1(p = 0.5)} - 1, \qquad (2)$$

  where $q(p = 50)$ is the value with an exceeding probability p = 1-F = 0.5, i.e. the 50-percentile of simulated discharges.

- RQ3, bias in the slope of the mid-segment as indicative of the average rate of change of daily discharge

$$RQ3 = \frac{\log_{10}\left(\frac{q_J(p=0.2)}{q_J(p=0.7)}\right)}{\log_{10}\left(\frac{q_1(p=0.2)}{q_1(p=0.7)}\right)} - 1, \qquad (3)$$

  where $q(p = 0.2)$ is the discharge with an exceeding probability p = 1-F = 0.2, i.e. the 80-percentile and $q(p = 0.7)$ is the discharge with an exceeding probability p = 1-F = 0.7, i.e. the 30-percentile.

- RQ4, bias in high-segment volumes, i.e. the difference in water volume for duration not exceeding a probability of 0.02:

$$RQ4 = \frac{\int_{p=0}^{0.02} q_J(p)dp}{\int_{p=0}^{0.02} q_1(p)dp} - 1 \qquad (4)$$

  where $0 \leq p \leq 0.02$ indicates the discharges with a probability of exceeding lower or equal to 2%, i.e. the maximum values.

- RQ5, bias in long-term baseflow:

$$RQ5 = \frac{\int_{p=0.7}^{1} \log_{10}\left(\frac{q_J(p)}{q_J(p=1)}\right) dp}{\int_{p=0.7}^{1} \log_{10}\left(\frac{q_1(p)}{q_1(p=1)}\right) dp} - 1 \quad (5)$$

where $0.7 \leq p \leq 1$ indicates the region of the lowest discharges; the index estimates the difference among the water volume individuated by the discharges with the highest exceedence probabilities.

After a first comparison among the simulated discharges, either in terms of monthly average discharges and FDCs (Fig.2 and Tab.2 in the Case Study section), the discharges resulting from the different simulations have been corrected with respect to the reference one using quantile-quantile method:

$$q_J^*(i) = F_1^{-1}(F_J(q_J(i))) \quad (6)$$

where $q_J(i)$ with J=2,3,4 is the i-th discharge of the J-th Run, F_J is the cumulative density function (hereinafter CDF) of simulation J, F_1^{-1} is the inverse of the CDF of the first simulation; $q_J^*(i)$ is the corrected discharge at day i for simulation J.

The Hazen plotting position has been assumed as distribution function for all the discharges:

$$F(q) = \frac{i - 0.5}{N}, \quad (7)$$

where i is the average rank and N the sample size. The main advantage of using an empirical CDF is that it fits the data but as drawback it does not allow to extrapolate values outside the sample range, in our case the range of the calibration period. The quantile-quantile correction technique has been applied splitting the discharge data into calibration, 1972-1990, and validation, 1991-2000, periods. The correction has been calibrated and validated at different aggregation scales (1) using all together the data (Run*J), (2) dividing the data into the four seasons DJF, MAM, JJA and SON (Run*J Seas) and (3) considering each month separately (Run*J Month). The behaviour of the different simulations within the calibration and validation periods and the results of the application of the quantile-quantile correction at yearly, seasonal and monthly scale are reported in Fig.s 3-6 and while values of RQ indices for the different cases are reported in Tab.s 3-6.

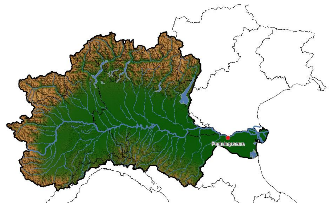

Figure 1:
The Po river basin and the main tributaries. The red dot indicates Pontelagoscuro site.

CASE STUDY

Po river is the longest in Italy with a length of 652 km from its source in Cottian Alps (at Pian del Re) to its mouth in the Adriatic Sea, in the north of Ravenna and is the largest Italian river with an average discharge of about 1500 m^3/s. The Po river basin is the widest in Italy and it covers an area of about 71000 km^2 including six regions: Lombardia, Piemonte, Liguria, Emilia-Romagna, Veneto, Valle d' Aosta, the autonomous province of Trento and about 3000 km^2 in Switzerland and France (Fig.1). As shown in Fig.1 the orography of the basin is complex due to the presence of the Alps at north and Apennines at south. The comparison among the monthly average areal precipitation over the period 1972-2000 provided by the four climate datasets is shown in Fig.2(a). The monthly average areal precipitation estimated using ERA40 Reanalysis (Run2) and CMCC-CM (Run4) as boundary conditions is overestimated from December to August (July for Run4) and underestimated from September to November, for both Run2 and Run4. The monthly average areal precipitation of Run3, that has the precipitation field statistically corrected, reduces the overestimation in December-July but amplifies the underestimation in Winter [28], see Fig.2(a). The monthly discharges reflect the behaviour of the precipitations, Fig.2(b); Run2 and Run4 overestimate discharges in Spring and Summer and underestimate them in Autumn when significant floods have been observed instead. Run3 reduces the discharge overestimation in almost all months but increases the autumnal underestimation. Run2, Run3 and Run4 all show a shift in the location of the spring peak while the autumnal peak falls in October correctly. A possible preliminary explanation of the shift from May to June of the peak could be related to the spatial distribution of precipitation and temperature in Winter/Spring since these two variables rule the snow accumulation/melting process and, as consequence, the timing of the spring peak. However, this point will be further investigated. The differences among the simulations are more evident comparing the FDCs and the RQ indices, see Fig.2(c) and Tab.2 respectively. In general, Run2 and Run4 overestimate the surveying (exceedance) probabilities, i.e. a prescribed discharge is less frequent in Run2 and Run4 than in Run1; the behaviour of Run3 is opposite, the surveying probability in underestimated with the exception of minimum discharges. The values of RQ indices agree with the above considerations: RQ1 and RQ2 are positive (overestimation of average and median discharges) for Run2 and Run4 and negative (underestimation) for Run3; the middle slope is quite well reproduced by all simulations (RQ3 ranges between -4.47% and +7.81%); high discharges are underestimated (RQ4 is negative for all simulations) and only Run2 (RQ5>0) overestimates the volume associated to the lowest discharges.

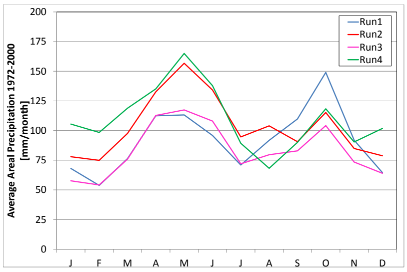

(a)

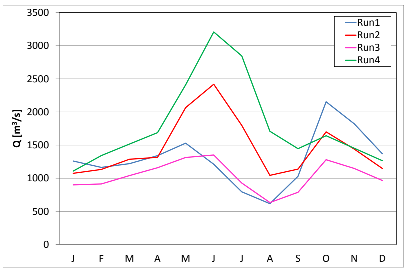

(b)

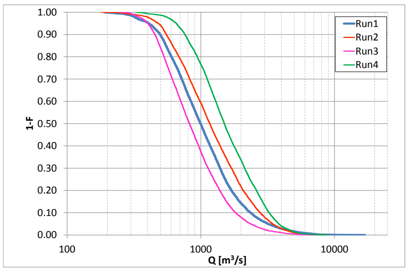

(c)

Figure 2:
Comparison among monthly average (a) areal precipitation and (b) discharges for the period 1972-2000. Panel (c) provides the comparison among the FDCs. Run1 is indicated in blue, Run2 in red, Run3 in magenta, and Run4 in green.

Table 2
FDC based indices (values are in percentage) for Run2, Run3, Run4 with respect to Run1 over the 1972-2000 period.

Index	Run2	Run3	Run4
RQ1	13.4	-19.9	39.9
RQ2	17.4	-17.4	50.7
RQ3	7.81	-4.47	-1.03
RQ4	-15.5	-31.0	-10.2
RQ5	19.1	-37.6	-8.85

Quantile-quantile correction of discharges

The differences in the precipitation fields in the four simulations considered, Fig.2(a), reflect into the discharges, Fig.s 2(b) and (c). A possibility to overcome such differences in discharges, without touching the climate input, is to apply a correction in probability as proposed in Eq.(6). We define 1972-1990 as calibration period and 1991-2000 as validation period before applying the quantile-quantile correction. Figure 3 reports a comparison among discharges of Run1 and those of Run2, Run3 and Run4 in the calibration (top) and validation (bottom) in terms of seasonality (left) and FDCs (right), Tab.3 provides the values of the RQ indices with respect to Run1 in calibration and validation periods. The comparison among monthly discharges in the calibration and validation periods, see Fig.s3(a) and (c) respectively, gives:

- Run1 an increase in discharges from October to January and a decrease in the other months;
- Run2 a behaviour similar to Run1 but the increase in autumnal discharge is less marked;
- Run3 discharges are characterised by a general decrease in all months;
- Run4 discharges show a behaviour similar to Run3.

Figures 3(b) and (d) report the comparison among FDCs in the calibration and validation periods, respectively, in both periods; Run2 and Run4 show a tendency to underestimate the rarity of discharges with respect to Run1 while Run3, in general, overestimates. Table 3 reports the RQ indices (values are in percentage) computed for the calibration and validation periods for Run2, Run3 and Run4 with respect to Run1 in the same periods. Within the calibration period, Run3 provides the best estimates for mean and median discharges (RQ1=-14.8% and RQ2=-14.3%, respectively) while Run4 show the maximum differences with Run1 (RQ1=45.6% and RQ2=52.7%, respectively); the slope of the FDC is similar in all the simulations while maximum discharges are well reproduced by Run2 (RQ4=-4.00%) and Run4 (RQ4=2.40%), Run3 underestimates them (RQ4=-20.7%) but it reproduces well the minimum discharges (RQ5=2.09%), while Run2 and Run4, in average, overestimates the minima. In the validation period, Run2 shows the most similar mean (RQ1=-2.78%) and median (RQ2=4.76%) discharge to Run1; the RQ3 index ranges between -9.94% (Run3) and 6.00% (Run2) with values comparable with those in the calibration period. All simulations underestimate the maximum discharges while minima are well simulated only by Run2 (RQ5=-4.48%). Note that the discharges of the reference simulation, Run1, show different ranges of variability in the calibration and the validation periods; in particular, discharges in the validation period are “more” extreme (i.e. higher and lower) than those in the calibration period, as shown in Fig.3(d). The RQ4 and RQ5 indices computed using as reference values the 1972-1990 discharges of Run1 and as “testing” data those in the validation period, have the values of 21.3% (in average, 6211 m^3/s vs 7721 m^3/s) and 31.35% (in average, 565 m^3/s vs 487 m^3/s), respectively, confirming the different range of

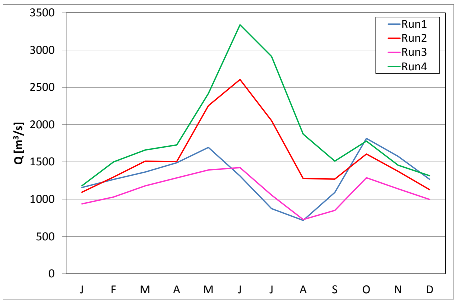

(a)

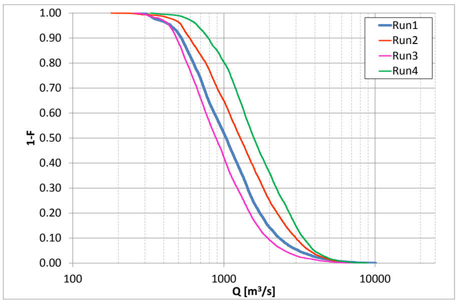

(b)

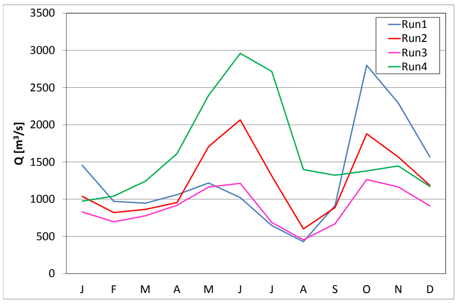

(c)

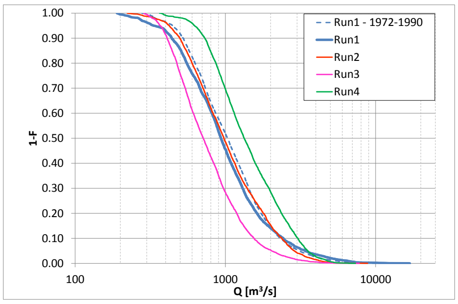

(d)

Figure 3:
Comparison among (a) monthly discharge and (b) FDCs of Run1, Run2, Run3 and Run4 for the calibration period (1972-1990) and (c) monthly discharge and (d) FDCs of Run1, Run2, Run3 and Run4 for the validation period (1991-2000).

Table 3
RQ indices, in percentage, for Run2, Run3 and Run4 for calibration (1972-1990) and validation (1991-2000) periods.

	Calibration			Validation		
Index	Run2	Run3	Run4	Run2	Run3	Run4
RQ1	21.7	-14.8	45.6	-2.78	-29.8	28.9
RQ2	24.1	-14.3	52.7	4.76	-23.7	42.8
RQ3	7.20	-5.37	-3.70	6.00	-9.94	-1.03
RQ4	-4.00	-20.7	2.40	-36.2	-47.9	-29.9
RQ5	88.2	2.09	41.7	-4.48	-54.2	-18.4

Table 4
RQ indices, values are in percentage, for Run*2, Run*3 and Run*4 for calibration (1972-1990) and validation (1991-2000) periods.

	Calibration			Validation		
Index	Run*2	Run*3	Run*4	Run*2	Run*3	Run*4
RQ1	-0.55	-0.56	-0.54	-21.3	-19.7	-13.7
RQ2	0.00	0.00	0.00	-16.3	-15.0	-10.8
RQ3	-0.29	-0.36	-0.39	-1.57	-1.31	1.19
RQ4	-4.70	-4.79	-4.61	-43.5	-37.4	-37.6
RQ5	-6.73	-6.52	-5.74	-50.9	-58.9	-45.4

discharge variability in calibration and validation periods.

The first application of Eq.(6) has been carried on considering all the data in the calibration period without separating them according to the season or the month of occurrence, thus the correction is more efficient on the FDCs than on the discharge seasonality, see Fig.4 and Tab.4. However, as discussed before, the range of Run1 discharge is larger in the validation period than in the calibration one and the Hazen plotting position does not allow to simulate values outside its calibration domain, thus Run*2, Run*3 and Run*4 may not perfectly reproduce the variability observed in Run1 discharges.

The content of Fig.4 and Tab.4 is analogue to Fig.3 and Tab.3. Run*2 and Run*4 in the calibration period, Fig.4(a), show a reduction in all the monthly discharges, while Run*3 is characterised by an increase. The spring shift persists as well as the underestimation of the peak values in October, Fig.4(a). At the same time, the FDCs, associated to discharges obtained from Run*2, Run*3 and Run*4, collapse on the one of Run1 as shown in Fig.4(b) and confirmed by the value of RQ indices in the left side of Tab.3. In the validation period, Fig.4(c), the monthly average discharges behave as in the calibration one; Run*2 and Run*4 reduce in all months becoming more close to the spring peak and overestimating more that the uncorrected simulations the autumnal values, while Run*3 shows a general increases in discharges but it is the one that follows better the discharges of Run1, with the exception of autumnal values where the underestimation is comparable with the one shown before the quantile-quantile correction, Fig.3(c). In the validation period, the corrected FDCs are closer than the uncorrected ones to Run1, Fig.3(c). The indices RQ1-RQ4 of Run*3 and Run*4 improves (the absolute values reduce) with respect to RQ1-RQ4 computed for Run3 and Run4, while indices computed for Run*2 are worste than those associated to Run2, right side of Tab.3.

Seasonal quantile-quantile correction of discharges

The quantile-quantile correction applied to the whole timeseries improves the similarity among the FDCs, however it is not sufficient to correctly reproduce the annual cycle of discharges, Fig.3. To better reproduce this feature, we applied the quantile-quantile correction dividing the data into four datasets, i.e. the CDFs to apply Eq.(6) are calibrated and validated splitting the dataset according to the season they occur, Winter (December, January, February), Spring (March, April, May), Summer (June, July, August) and Autumn (September, October, November). The seasonally corrected simulations are labelled Run*J Seas. The results of the seasonal correction are summarised

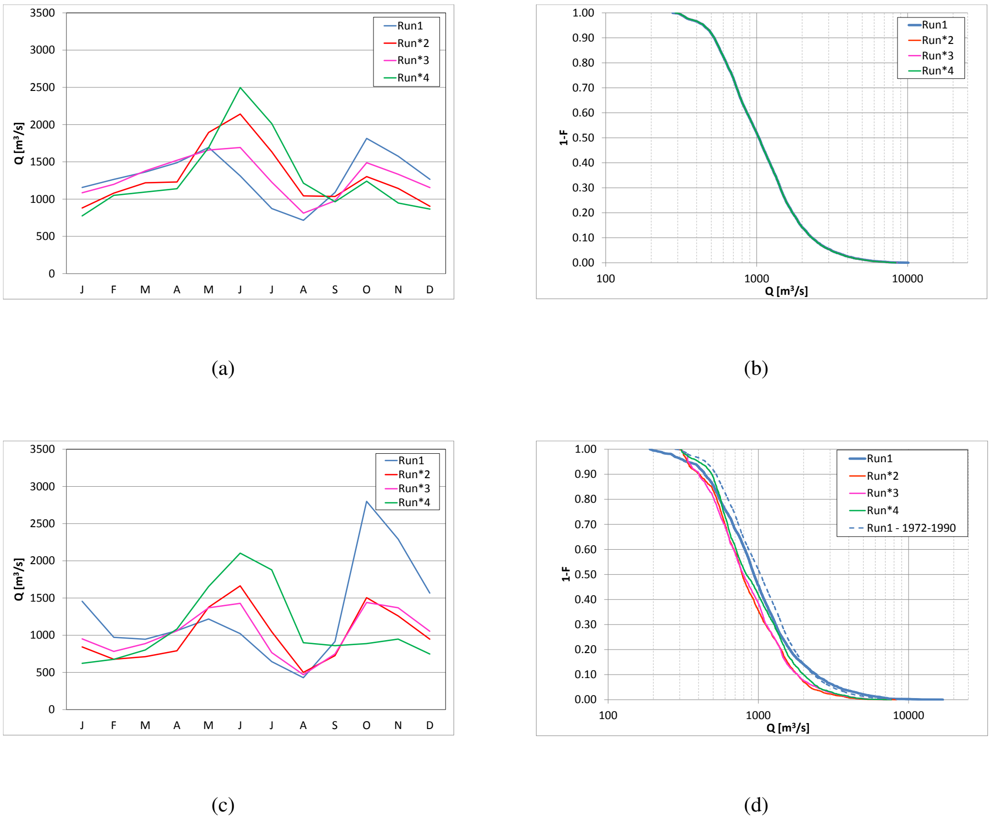

Figure 4:
Same comparison of Fig.3 but among Run1 and Run*2, Run*3 and Run*4.

Table 5
RQ indices, in percentage, for Run*2 Seas, Run*3 Seas and Run*4 Seas for calibration (1972-1990) and validation (1991-2000) periods.

	Calibration			Validation		
Index	Run*2 Seas	Run*3 Seas	Run*4 Seas	Run*2 Seas	Run*3 Seas	Run*4 Seas
RQ1	-0.48	-0.50	-0.48	-15.8	-16.6	-12.2
RQ2	-0.02	0.01	-0.02	-13.9	-14.2	-5.20
RQ3	-0.42	-0.54	-0.47	-5.72	-1.75	-0.90
RQ4	-3.63	-3.79	-3.65	-31.8	-30.9	-34.4
RQ5	-0.93	-0.85	-1.09	-54.45	-56.0	-37.0

Table 6
RQ indices, in percentage, for Run*2 Month, Run*3 Month and Run*4 Month for calibration (1972-1990) and validation (1991-2000) periods.

	Calibration			Validation		
Index	Run*2 Month	Run*3 Month	Run*4 Month	Run*2 Month	Run*3 Month	Run*4 Month
RQ1	-0.61	-0.57	-0.58	-15.2	-16.6	-11.6
RQ2	-0.09	-0.03	-0.07	-12.7	-13.9	-5.30
RQ3	-0.70	-0.72	-0.76	-1.50	2.51	-5.36
RQ4	-3.93	-3.75	-3.83	-30.7	-33.2	-29.1
RQ5	-0.43	-0.66	-0.40	-51.4	-50.1	-34.4

for calibration and validation periods, in terms of monthly discharges and FDCs, Fig.5, and RQ indices, Tab.5. In the calibration period, Run*3 Seas correctly reproduces Run1 average monthly discharges and also Run*2 and Run*4 show a good agreement with Run1; for all the simulations the spring peak is correctly located in May and the peak in October is caught, Fig.5(a). The seasonally corrected FDCs collapse on the one of Run1, Fig.5(b). Values of RQ indices, reported on the left side of Tab.5, confirm the good agreement among the FDCs with a light underestimation of maximum discharges (the average value of RQ4 index is about -3.7%). Within the validation period, the average monthly discharges of Run*2 Seas and Run*3 Seas are similar to those of Run1 and Run*2 Seas better reproduces the average discharge of October, even if the underestimation persists, Fig.5(c). The FDCs of corrected simulations fall on the left of the FDC of Run1 for almost all the levels of probability; only the probability of the lowest discharges is overestimated, Fig.5(d). The values of RQ indices, reported on the right side of Tab.5, are slightly better than those computed for Run*2 , Run*3 and Run*4 in the same period (Tab.4).

Monthly quantile-quantile correction of discharges

The application at monthly scale of Eq.(6) guarantees that, in the calibration period, the monthly average discharges are correctly estimated, Fig.6(a), as well as the FDCs, Fig.6(b). The RQ indices reported in Tab.6 confirm the similarity among the FDCs and the small underestimation of the maximum discharges (RQ4 ranges from -3.75% to -3.93%) as noted also in the seasonal application of the quantile-quantile correction. Within the validation period, Run*2 Month and Run*3 Month perform better than Run*4 Month in reproducing the annual discharge cycle, however the average discharge in October is still underestimated, Fig.6(c). As in previous cases, the FDCs differs specially in extreme values (Fig.6(d) and Tab.6(right)), the highest discharges are underestimated of about 30% (RQ4 index) and the underestimation of the volume associated to the lowest discharges ranges between -51.4% and -34.4%. However, the values of RQ4 and RQ5 indices are influenced by the difference among Run1 discharges in the calibration and validation periods; if the RQ4 and RQ5 indices for the validation period are computed with respect to the discharges of Run1 from the calibration period, they range between -16% and -24% for RQ4, and -28% and -36% for RQ5.

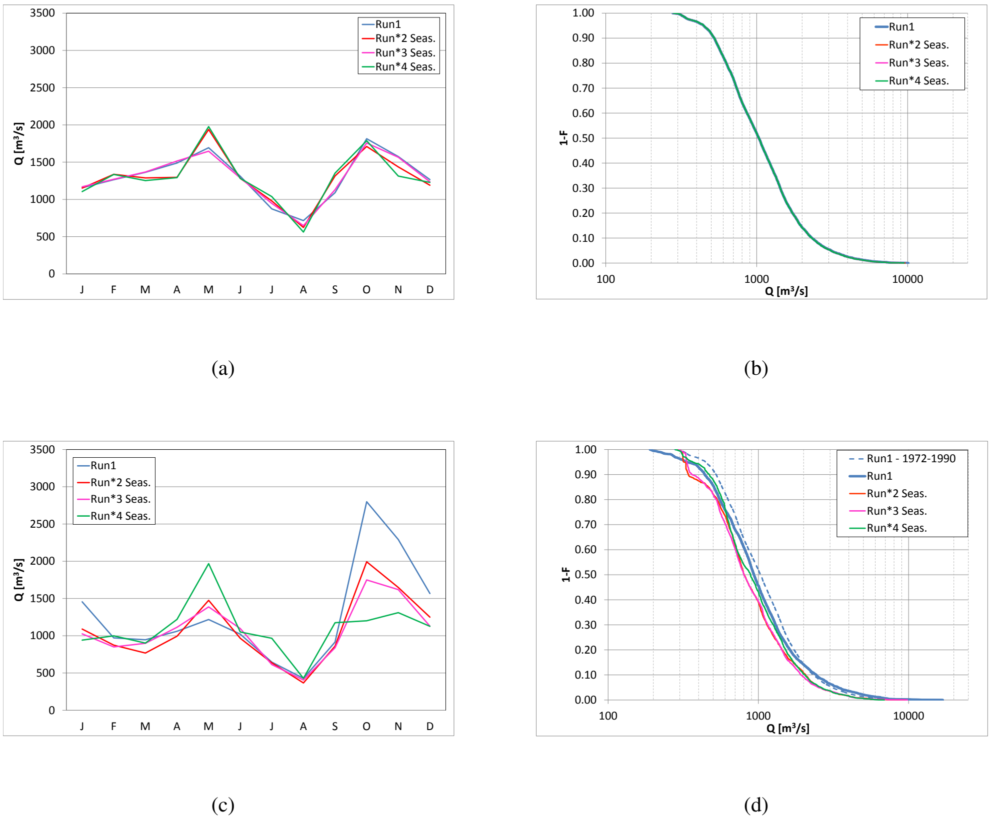

Figure 5:
Same comparison of Fig.3 but among Run1 and Run*2 Seas, Run*3 Seas and Run*4 Seas

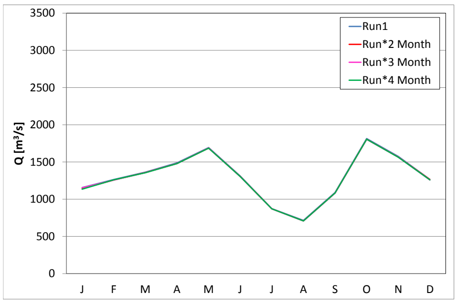

(a)

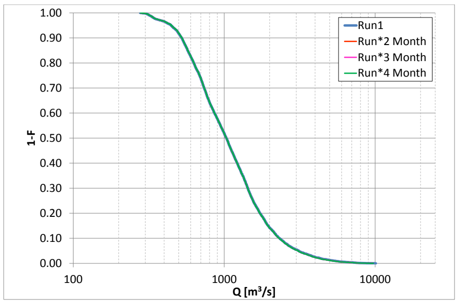

(b)

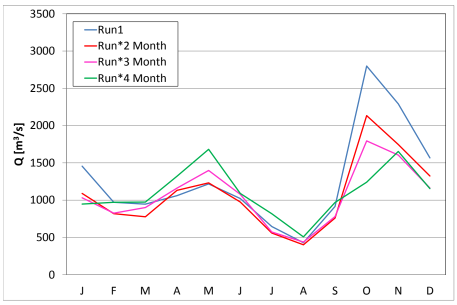

(c)

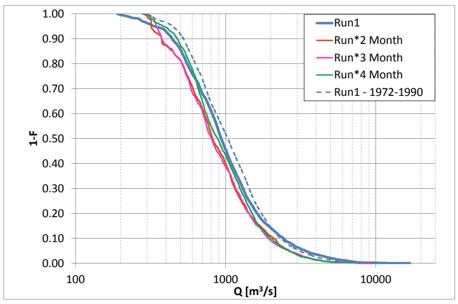

(d)

Figure 6:
Same comparison of Fig.3 but among Run1 and Run*2 Month, Run*3 Month and Run*4 Month.

CONCLUSIONS

The climate-hydrological simulations performed over the period 1971-2000 shows a difference in the precipitation partitioning in time and in the overall volume depending on the climate simulations considered. This variability is reflected in the river discharge seasonality. The comparison of monthly average discharges shows that the Po river discharge seasonality is mostly reproduced, but autumnal discharges are highly underestimated due to a scarcity of precipitation and a shift in maximum discharges from May to June is detected. The shift is probably related to the snow accumulation/melting processes and this issue will be further analysed. The application of quantile-quantile corrections at different aggregation scale helps to improve the similarity among discharge seasonality and flow-duration curves as confirmed by the values of the RQ indices in the calibration (1972-1990) and validation (1991-2000) periods. However, the use of the Hazen plotting position limits the possibility to reproduce the most extreme values observed in the validation period. The use of a continuous CDF to describe the discharge data should improve the results of the quantile-quantile correction technique, it will be tested in next months and results will be presented in a forthcoming paper. As alternative to the proposed quantile-quantile correction of discharges, statistical corrections can be applied to precipitation and temperature obtained from the RCM to provide statistically correct climate inputs to the hydrological/hydraulic models [23, 22]. Simulations driven by a statistically correct climate are expected to provide discharges close to those coming from the reference simulation. The results of this approach will be also presented in a forthcoming paper. However, the quantile-quantile correction applied directly to the discharges is a possible way to remove the overall uncertainties introduced by different components of modelling chains, even in absence of climate data to validate/correct the precipitation input to the hydrological/hydraulics models.

Bibliography

[1] *The RCP Greenhouse Gas Concentrations and their Extensions from 1765 to 2500*, chapter Climatic Change. 2011.

[2] S. Blenkinsop and H.J. Fowler. Changes in European drought characteristics projected by the PRUDENCE regional climate models. *Int. J. Climatol.*, 27:1595 – 2610, 2007.

[3] L. Casicci, C. Ioiò, and S. Pecora. An operational system for the Po flood forecasting in Italy. In *7th International Conference on Hydroinformatics HIC, Nice, France*, 2006.

[4] M. C. Casper, G. Grigoryan, O. Gronz, O. Gutjahr, G. Heinemann, R. Ley, and A. Rock. Analysis of projected hydrological behavior of catchments based on signature indices. *Hydrology and Earth System Sciences*, 16(2):409–421, 2012.

[5] J.H. Christensen, B. Hewitson, A. Busuioc, A. Chen, X. Gao, I. Held, R. Jones, R.K. Kolli, W.-T. Kwon, R. Laprise, V. Maga na Rueda, L. Mearns, C.G. Menéndez, J. Räisänen, A. Rinke, A. Sarr, and P. Whetton. *Climate Change 2007: The Physical Science Basis. Contribution of Working Group I to the Fourth Assessment Report of the Intergovernmental Panel on Climate Change*, chapter Regional Climate Projections. Cambridge University Press, Cambridge, United Kingdom and New York, NY, USA, 2007.

[6] N.S. Christensen, A.W. Wood, N. Voisin, D.P. Lettenmaier, and R.N. Palmer. The effects of climate change on the hydrology and water resources of the Colorado river basin. *Climate Change*, 62:337 – 363, 2004.

[7] H.J Fowler and C.G Kilsby. Future increases in UK water resources projected by a regional climate model. *Hydrology: Science & practice for the 21st century*, 1:15 – 21, 2004.

[8] M.R. Haylock, N. Hofstra, A.M.G. Klein Tank, E.J. Klok, P.D. Jones, and M. New. A european daily high-resolution gridded data set of surface temperature and precipitation for 1950-2006. *J. Geophys. Res.*, 113(D20119), 2008.

[9] M. Herbst, H. V. Gupta, and M. C. Casper. Mapping model behaviour using self-organizing maps. *Hydrology and Earth System Sciences*, 13(3):395–409, 2009.

[10] Y. Hirabashi, S. Kanae, S. Emori, T. Oki, and M. Kimoto. Global projections of changing risks of floods and droughts in a changing climate. *Hydrological Sciences Journal*, 53(4):754 – 772, 2008.

[11] Delft Hydraulics. River basin planning and management simulation program. In A. Voinov, A.J. Jakeman, and A.E. Rizzoli, editors, *Proceedings of the iEMSs Third Biennial Meeting: Summit on Environmental Modelling and Software*. International Environmental Modelling and Software Society, 2006.

[12] Z. Liu and E. Todini. Towards a comprehensive physically-based rainfall-runoff model. *Hydrol. Earth Syst. Sc.*, 6(5):859–881, 2002.

[13] M. Montesarchio, M.P. Manzi, L. Cattaneo, E. Bucchignani, and P. Mercogliano. Performance evaluation of a regional climate simulation with COSMO-CLM in the Alpine space. *CMCC - Research Paper RP00137*, 2012.

[14] B. Rockel, A. Will, and A. Hense. The regional climate model COSMO-CLM (CCLM). *Meteorologische Zeitschrift*, 17(4):347–348, 2008.

[15] E. Scoccimarro, S. Gualdi, A. Bellucci, A. Sanna, P.G. Fogli, E. Manzini, M. Vichi, P. Oddo, and A. Navarra. Effects of tropical cyclones on ocean heat transport in a

high resolution coupled general circulation model. *Journal of Climate*, 24:4368–4384, 2011.

[16] O. Seidou, A. Ramsay, and I. Nistor. Climate change impacts on extreme floods I: combining imperfect deterministic simulations and non-stationary frequency analysis. *Nat. Hazard*, 61:647 – 657, 2012.

[17] O. Seidou, A. Ramsay, and I. Nistor. Climate change impacts on extreme floods II: improving flood future peaks simulation using non-stationary frequency analysis. *Nat. Hazard*, 60:715 – 726, 2012.

[18] A.H. te Linde, J.C.J.H. Aerts, A.M.R. Bakker, and J.C.J. Kwadijk. Simulating low probability peak discharges for the Rhine basin using resampled climate modeling data. *Water Resour. Res.*, 46:W04512, 2010.

[19] A.H. te Linde, P. Bubeck, J.E.C. Dekkers, H. de Moel, and J.C.J.H. Aerts. Future flood risk estimates along the river Rhine. *NHESS*, 11:459 – 473, 2011.

[20] M. Turco, P. Quintan-Seguí, M.C. Llasat, S. Herrera, and J.M. Gutiérrez. Testing MOS precipitation downscaling for ENSEMBLES regional climate models over Spain. *Journal of Geophysical Research*, 116:D18109, 2011.

[21] M. Turco, A.L. Zollo, G. Rianna, L. Cattaneo, R. Vezzoli, and P. Mercogliano. Post-processing methods for COSMO-CLM precipitation over italy. *CMCC Research Paper*, RP0171, 2013.

[22] M. Turco, A.L. Zollo, V. Rillo, and P. Mercogliano. GCM driven COSMO-CLM post-processed precipitation over Italy: control and future scenarios. *CMCC - Research Paper*, RP0179, 2013.

[23] M. Turco, A.L. Zollo, R. Vezzoli, C. Ronchi, and P. Mercogliano. Daily precipitation statistics over the Po basin: observation and post-processed RCM results. In *SISC First Annual Conference, Lecce 2013*, 2013.

[24] S.M. Uppala, P.W. Kallberg, A.J. Simmons, U. Andrae, V.D. Bechtold, M. Fiorino, J.K. Gibson, J Haseler, A. Hernandez, G.A. Kelly, X. Li, K. Onogi, S. Saarinen, N. Sokka, R.P. Allan, E. Andersson, K. Arpe, M.A. Balmaseda, A.C.M. Beljaars, L. Van de Berg, J. Bidlot, N. Bormann, S. Caires, F. Chevallier, A. Dethof, M. Dragosavac, M. Fisher M., M. Fuentes, S. Hagemann, E. Holm, B.J. Hoskins, L. Isaksen, P.A.E.M. Janssen, R. Jenne, A.P. McNally, J.F. Mahfouf, J.J. Morcrette, N.A. Rayner, R.W. Saunders, P. Simon, A. Sterl, K.E. Trenberth, A. Untch, D. Vasiljevic, P. Viterbo, and J. Woollen. The ERA40 re-analysis. *Quart. J. Roy. Meteor. Soc.*, 612:2961–3012, 2006.

[25] K. K. Yilmaz, H. V. Gupta, and T. Wagener. A process-based diagnostic approach to model evaluation: Application to the nws distributed hydrologic model. *Water Resour. Res.*, 44:W09417, 2008.

[26] D. Zanchettin, P. Traverso, and M. Tomasino. Po river discharge: a preliminary analysis of a 200-year time series. *Climatic Change*, 89:411–433, 2008.

[27] A.L. Zollo, P. Mercogliano, M. Turco, R. Vezzoli, G. Rianna, E. Bucchignani, M.P. Manzi, and M. Montesarchio. Architectures and tools to analyse the impacts of climate change on hydrogeological risk on Mediterranean area. *CMCC Research Paper*, RP0129, 2012.

[28] A.L. Zollo, M. Montesarchio, M.P. Manzi, L. Cattaneo E. Bucchignani, and P. Mercogliano. Assessment of COSMO-CLM performances in simulating the past climate of Italy. *CMCC Research Paper*, RP0145, 2012.